

Research Article

Multilevel Clustering-Evolutionary Random Support Vector Machine Cluster Algorithm-Based Functional Magnetic Resonance Imaging in Diagnosing Cerebral Ischemic Stroke

Kun Fan , Ting Zhang , and Weihong He 

Department of Radiology, The Second Affiliated Hospital, Hengyang Medical School, University of South China, Hengyang, Hunan 421001, China

Correspondence should be addressed to Weihong He; hwh@usc.edu.cn

Received 25 June 2021; Revised 2 August 2021; Accepted 13 August 2021; Published 25 September 2021

Academic Editor: Gustavo Ramirez

Copyright © 2021 Kun Fan et al. This is an open access article distributed under the Creative Commons Attribution License, which permits unrestricted use, distribution, and reproduction in any medium, provided the original work is properly cited.

This study was to explore the value of the blood oxygenation level dependent-functional magnetic resonance imaging (BOLD-fMRI) image classification based on the multilevel clustering-evolutionary random support vector machine cluster (MCRSVMC) algorithm in the diagnosis and treatment of patients with cognitive impairment after cerebral ischemic stroke (CIS). The MCRSVMC algorithm was optimized using a clustering algorithm, and it was compared with other algorithms in terms of accuracy (ACC), sensitivity (SEN), and specificity (SPE) of classifying the brain area images. 36 patients with cognitive impairment after CIS and nondementia patients were divided into a control group (drug treatment) and an intervention group (drug + acupuncture) according to different treatment methods, with 18 cases in each group. The changes in regional homogeneity (ReHo) of BOLD-fMRI images and the differences in scores of the Montreal Cognitive Assessment Scale (MoCA), scores of Loewenstein Occupational Therapy Cognitive Assessment (LOTCA), and scores of Functional Independence Measure (FIM) between the two groups of patients were compared before and after treatment. The results revealed that the average classification ACC, SEN, and SPE of the MCRSVMC algorithm were $84.25 \pm 4.13\%$, $91.07 \pm 3.51\%$, and $89 \pm 3.96\%$, respectively, which were all obviously better than those of other algorithms ($P < 0.01$). When the number of support vector machine (SVM) classifiers and the number of important features were 410 and 260, respectively, the classification ACC of MCRSVMC algorithm was 0.9429 and 0.9092, respectively. After treatment, the MoCA score, LOTCA score, and FIM score of the patients in the intervention group were higher than those of the control group ($P < 0.05$). The ReHo values of the right inferior temporal gyrus and right inferior frontal gyrus of patients in the intervention group were much higher than those of the control group ($P < 0.05$). It indicated that the classification ACC, SEN, and SPE of the magnetic resonance imaging (MRI) based on the MCRSVMC algorithm in this study were greatly improved, and the acupuncture method was more effective in the treatment of patients with cognitive dysfunction after CIS.

1. Introduction

Cerebral ischemic stroke (CIS) is the most common type of stroke. In China, nearly 2 million CIS patients are newly added every year, and about 75% of patients after CIS suffer from different degrees of cognitive dysfunction [1]. At present, the mild cognitive dysfunction is mainly diagnosed by scale examination and imaging examination. Clinical imaging methods for CIS mainly include cranial CT, ECG (electrocardiogram), and cranial MRI. Cranial CT scan is a

conventional and the most important diagnostic examination method for nervous system diseases, with the advantages of high resolution, accurate diagnosis, and low cost. It is mainly used to exclude cerebral hemorrhage, brain tumor, and other diseases, but the display effect for soft tissue is not very good. ECG is used to assess whether the patient is complicated with heart disease, but the development of ACI cannot be directly judged. Resting-state functional magnetic resonance imaging (rs-fMRI) is widely used in the clinical diagnosis of cognitive dysfunction after CIS due to its

advantages of noninvasiveness, nonradiation, reproducibility, and quantification. rs-fMRI is very sensitive to the spontaneous low-frequency oscillations of the brain, and it can detect the strength of the signal of blood oxygenation level dependent (BOLD), so as to reflect the unique active brain areas of the subject at the resting state [2]. BOLD signal is closely related to the synchronization of neural activity and is considered to reflect the input and processing of neural information in the local brain region. Its formation is based on the change of the ratio of oxyhemoglobin to deoxyhemoglobin in cerebral blood flow.

With the continuous development of data mining technology, multilayer network methods based on machine learning and deep learning have been applied to the parameter identification of proton exchange membrane fuel cells [3], design on evacuation methods in public places [4], and medical image recognition and segmentation [5]. However, machine learning shows poor performance in the recognition of multivariate or nonlinear decision boundary in data processing of the functional magnetic resonance imaging (fMRI) and is prone to overfitting. Moreover, the machine learning algorithm has a poor processing effect on small samples and high-dimensional and high-noise data. The network structure of the deep learning model is relatively complicated, and there are disadvantages such as high difficulty in reverse analysis, insensitivity of high dimensionality, and nonrobustness in the process of fMRI data processing [6]. Support vector machine (SVM) clusters take advantage of the SVM algorithm in fMRI data processing, randomly extract some features to build multiple SVM base classifiers, and finally make classification decisions on the test samples by means of equal weight voting. Studies have pointed out that the classification accuracy (ACC) of SVM clusters for Alzheimer's patients and normal people is as high as 74.44% [7]. At present, SVM clusters still have the disadvantages of ignoring the redundancy among SVM individuals in fMRI data processing, and the effectiveness of the SVM base classifier cannot be determined [8].

In summary, the processing of fMRI data by MCRSVMC still needs to be further optimized. Therefore, the MCRSVMC algorithm was optimized, and a brain region classification model was established in this study. The nondementia patients with cognitive dysfunction after CIS were selected as the research objects, and the brain classification model based on MCRSVMC algorithm was used to evaluate the two different therapeutic effects of cognitive dysfunction in CIS patients, aiming to provide a reference basis for the clinical diagnosis and treatment of CIS patients.

2. Materials and Methods

2.1. Research Objects and Grouping. 36 nondementia inpatients with cognitive dysfunction after CIS who were admitted to the hospital from February 2019 to December 2020 were selected as the research objects, including 20 males and 16 females who were 50–80 years old (with the average age of 63.59 ± 5.42 years). The inclusion criteria were defined as follows: patients with clear consciousness and with the course of disease of ≤ 1 year; patients who were right-handed;

patients whose diagnosis was in line with the CIS diagnosis and treatment standards set by the Chinese Medical Association and the Montreal Cognitive Assessment Scale (MoCA) score < 26 points; and patients with no contraindications to fMRI examination. The exclusion criteria were defined as follows: patients with impaired consciousness, severe vision, and hearing and speech impairments; patients who were unable to complete the health assessments; patients with multiple sclerosis or brain tumors and other brain diseases; patients with cognitive dysfunction caused by other reasons, such as Alzheimer's disease and Lewy body dementia; and patients with tumors, severe organs, endocrine system, and other diseases. According to different treatment methods, they were rolled into a control group (drug treatment) and an intervention group (drug + acupuncture), with 18 cases in each group. The process had been approved by the ethics committee of the hospital, and all subjects included in the study had signed the informed consent forms.

2.2. Establishment of the Brain Classification Model Based on the MCRSVMC Algorithm. Clustering displays the inherent properties and laws of the data by learning from unlabeled samples. The SVM cluster uses multiple SVM classifiers for combined prediction, and its generalization performance is much better than a single SVM [9]. In this study, an automatic anatomical labeling (AAL) prior template was used to divide the brain region to obtain 90 regions of interest (ROIs). The degree value Y_i of brain area i reflected the status and role of a certain brain area in the entire brain area network. The degree value Y_i can be expressed as follows:

$$Y_i = \sum_{j=1}^n x_{ij}. \quad (1)$$

In the equation above, $i \neq j$, and n represents the number of brain areas. If there was an edge from brain area i to brain area j , then $x_{ij} = 1$; if there was no edge from brain area i to brain area j , then $x_{ij} = 0$.

The shortest distance for the information of brain area i to reach brain area j was called the shortest path D_{ij} , which could be calculated with equation (2), in which y_{ij} represented any distance between brain area i and brain area j :

$$D_{ij} = \min(y_{ij}). \quad (2)$$

Local efficiency E_i represents the ability of information exchange between neighbor nodes of brain area i , and its expression is given as follows:

$$E_i = \frac{1}{z_i(z_i - 1)} \sum_{i \neq j \in \mu_i} \frac{1}{D_{ij}}. \quad (3)$$

In the above equation, z_i represents the number of neighbors of brain area i , and μ_i represents the graph composed of all brain areas directly connected to brain area i .

The clustering coefficient G_i represents the possibility that the neighbors of brain area i were neighbors to each

other. It could be expressed as equation (4), in which e refers to the number of edges that actually exist between neighbors of brain area i :

$$G_i = \frac{e}{G_{z_i}^z} = \frac{2e}{z_i(z_i - 1)}. \quad (4)$$

To improve the generalization performance of the model, a clustering algorithm was introduced in the MCRSVMC algorithm to eliminate weak learners with low ACC and high similarity (SIM). In the process of clustering, a variety of clustering methods are used to control the convergence speed of clustering. For a given dataset $\{a_1, a_2, \dots, a_l\}$, its corresponding individual learner could be defined as $\{SVM_1, SVM_2, \dots, SVM_n\}$; then, the classification of an SVM learner can be expressed as follows:

$$f_i(a) = \begin{cases} 1, & SVM_i \text{ correct classification,} \\ 0, & SVM_i \text{ misclassification.} \end{cases} \quad (5)$$

It was supposed that b was the number of samples that can be correctly classified by SVM_i and SVM_j in the dataset; c was the number of samples that were correctly classified by SVM_i but incorrectly classified by SVM_j ; d referred to the number of samples that were classified incorrectly by SVM_i but correctly classified by SVM_j ; and e represented the number of samples that were classified incorrectly by both SVM_i and SVM_j . Then, b , c , d , and e can be expressed as the following equations:

$$b = \sum_{k=1}^l D[f_{(k,i)} = f_{(k,j)} = 1], \quad (6)$$

$$c = \sum_{k=1}^l D[(f_{(k,i)} = 1) \wedge (f_{(k,j)} = 0)], \quad (7)$$

$$d = \sum_{k=1}^l D[(f_{(k,i)} = 0) \wedge (f_{(k,j)} = 1)], \quad (8)$$

$$e = \sum_{k=1}^l D[(f_{(k,i)} = f_{(k,j)} = 0)]. \quad (9)$$

In equations (6)–(9), $D[\]$ represents the indicator function. The dual optimization Q_{ij} between SVM_i and SVM_j can be expressed as equation (10), where the value range of Q_{ij} could be calculated:

$$Q_{ij} = \frac{be - cd}{be + cd}. \quad (10)$$

The correlation coefficient R_{ij} between SVM_i and SVM_j was a measure of the degree of correlation between two learners, and its calculation method can be expressed as shown in equation (11), where the value range of R_{ij} was $[-1, 1]$, both R_{ij} and Q_{ij} were the same as positive and negative, and $R_{ij} \leq Q_{ij}$.

$$R_{ij} = \frac{be - cd}{\sqrt{(b+c)(b+d)(e+c)(e+d)}}. \quad (11)$$

The kappa statistic was a coefficient reflecting the degree of consistency between two learners, and the kappa statistic (K_{ij}) between SVM_i and SVM_j can be expressed as the following equation:

$$K_{ij} = \frac{2(bd - ce)}{(b+c)(b+d)(e+c)(e+d)}. \quad (12)$$

The distance measure (Dis_{ij}) between SVM_i and SVM_j represents the proportion of the samples with inconsistent classification results of the two learners in the total samples, and it could be calculated with the following equation:

$$Dis_{ij} = \frac{c+d}{b+c+d+e}. \quad (13)$$

In this study, the brain region classification based on the MCRSVMC algorithm mainly involved the multilevel clustering evolution process. For the brain dataset D , it was classified into a collection and a test set, and the collection mainly includes two parts: a training set and a verification set. The training set in the dataset D was to train the SVM-based learner, obtain the classification result of the SVM according to the verification set, and perform clustering according to the SIM measurement index of the classification result. It could be divided into g clusters, and the individual learner with the highest classification ACC was selected from each cluster to be the representative member. After multiple clustering processes, the number of clusters would gradually decrease. When the number of clusters in the model reached the set threshold h , the model calculation would stop. The SVM classifier composed of the highest ACC SVM was selected from h clusters to form a new cluster. The flowchart of brain area classification based on MCRSVMC algorithm is shown in Figure 1.

2.3. Application of the Brain Area Classification Model Based on the MCRSVMC Algorithm in CIS Diagnosis. For the rs-fMRI technology to obtain fMRI images, it was preprocessed through time correction, head movement correction, image standardization, spatial smoothing, linear drift removal, filter processing, and removal of covariates. The preprocessed fMRI image was compared with the AAL atlas to establish the corresponding functional connection matrix, and the fMRI image was classified by the brain region classification model of the MCRSVMC algorithm to obtain the optimal feature subset, acquiring the abnormal brain area corresponding to the optimal feature subset. Figure 2 shows the application process of the brain region classification model based on the MCRSVMC algorithm in the diagnosis of nondementia patients with cognitive dysfunction after CIS.

ACC, SEN, and SPE were adopted to evaluate the brain classification performance of the MCRSVMC algorithm in this study. ACC referred to the proportion of samples that were correctly classified among all samples, SEN represented the proportion of all positive samples that were correctly classified, and SPE referred to the proportion of all negative samples that were correctly classified.

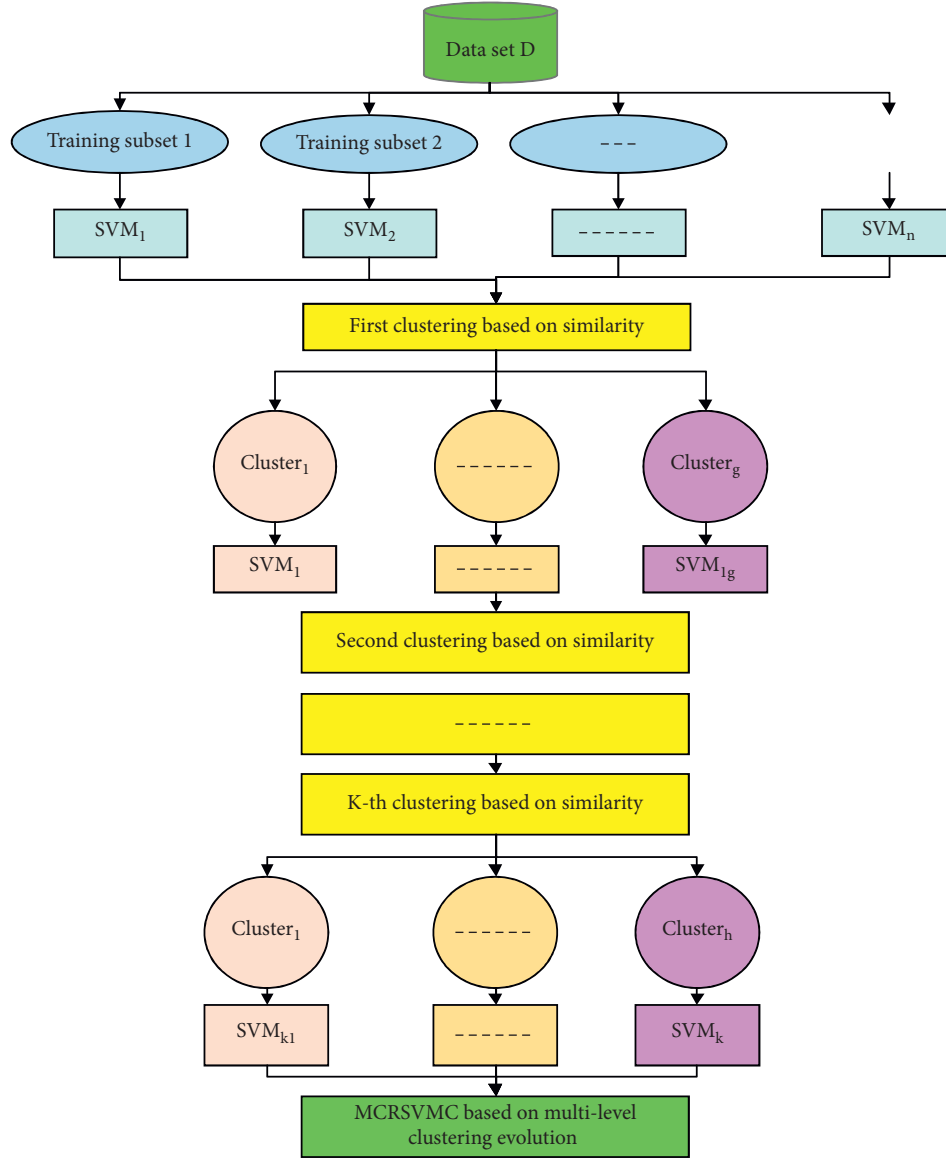


FIGURE 1: The flowchart of brain area classification based on the MCRSVMC algorithm.

$$ACC = \frac{TP + TN}{TP + FP + FN + TN}, \quad (14)$$

$$SE = \frac{TP}{TP + FN}, \quad (15)$$

$$SP = \frac{TN}{TN + FP}. \quad (16)$$

In equations (14)–(16), TP represents the number of true positive samples; FP represents the number of false positive samples; FN represents the number of false negative samples; and TN represents the number of true negative samples.

2.4. BOLD-fMRI Scan and Treatment of CIS Patients. In this study, the patient was scanned using a Siemens MAGNETOM Skyra 3.0 magnetic resonance imaging system. All CIS

patients underwent BOLD-fMRI scans before and after treatment in a resting state. The T1-weighted image (T1WI) was performed as follows. The spin echo sequence was adopted with 33 layers of the axial plane, and the scanning parameters were given as follows: the repetition time (TR) was 2,000 ms, echo time (TE) was 30 ms, field of view (FOV) was 24 cm × 24 cm, matrix was 64 × 64, reversal time was 750 ms, layer thickness was 3.0 mm, and layer interval was 0.6 mm. The fMRI scan was performed with the following operations. The planar echo imaging sequence was adopted to scan the resting-state functional image on the same plane as the T1 image. The scanning parameters were set as follows: TR was 2,000 ms, TE was 30 ms, reversal angle was 90 degrees, FOV was 24 cm × 24 cm, matrix was 64 × 64, layer number was 30, and layer thickness was 5 mm. The changes in regional homogeneity (ReHo) before and after treatment were compared between the two groups.

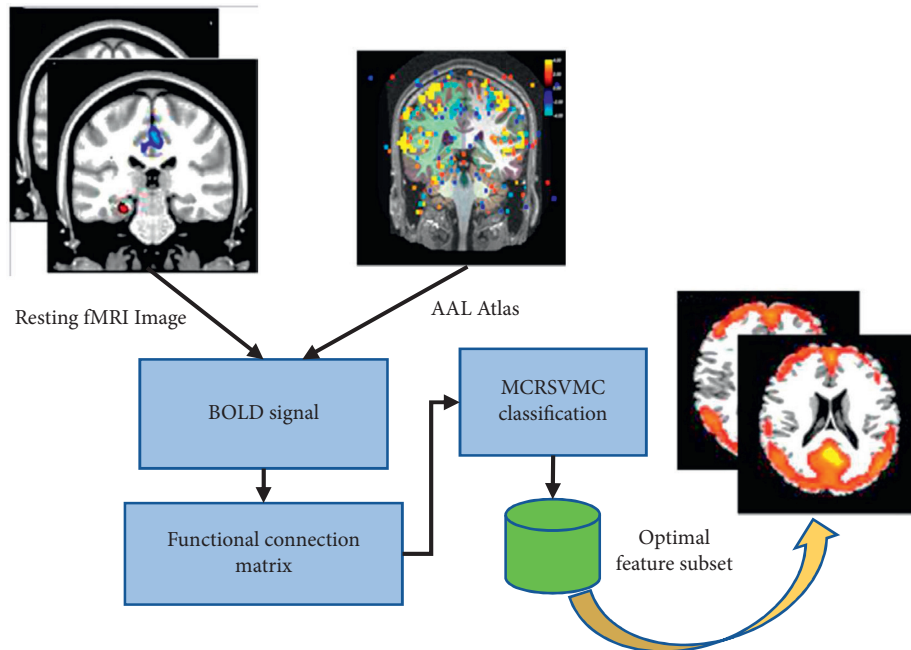


FIGURE 2: Flowchart of applying the brain area classification based on the MCRSVMC algorithm in CIS diagnosis.

2.5. Therapeutic Regimen. Patients in the control group were treated with conventional medical drugs. All patients were treated with 5 mg folic acid tablets + 500 ug mecobalamin tablets + 610 mg vitamin B, three times a day; in addition, drugs to improve the cognitive function (5 mg donepezil/time/day) were given. Patients in the intervention group were given with electrical acupuncture stimulation on the basis of the aforementioned drug treatments. They were placed in a supine position, routinely disinfected the treatment area, and quickly inserted acupuncture needles with 0.3 mm × 40 mm. Each point was punctured at a level of 0.5–0.8 inch. The needle was twisted for 200 times/min and left for 6 hours. The patients were treated for 6 days a week, with 1 day of rest for a concussive treatment for one month.

2.6. Statistical Methods. The test data were processed using SPSS 19.0 statistical software. The measurement data were expressed as mean ± standard deviation ($\bar{x} + s$), and the t -test was adopted for comparison; the count data were expressed in the form of percentage, and the χ^2 test was used. $P < 0.05$ indicated that the difference was statistically significant.

3. Results

3.1. Comparison on Classification Performances. The MCRSVMC classification algorithm in this study was compared with the random forest (RF), probabilistic neural network (PNN), naive Bayes classifier (NBC), and K -nearest neighbor (KNN) in terms of classification ACC, SEN, and SPE, and the results are given in Figure 3. RF, SVM, PNN, NBC, and KNN were all machine learning algorithms.

The average classification ACC, SEN, and SPE of the MCRSVMC algorithm were $84.25 \pm 4.13\%$, $91.07 \pm 3.51\%$,

and $89 \pm 3.96\%$, respectively, which were all much better than those of other algorithms ($P < 0.01$).

Figure 4 shows the image processing effects of different algorithms. It can be clearly concluded that MCRSVMC algorithm had the best enhancement effect on cranial fMRI images, which was better than other algorithms.

3.2. Selection of the Optimal Number of Classifiers and Optimal Feature Subset. The number of SVM classifiers corresponding to the highest ACC of the MCRSVMC algorithm was the optimal number of base classifiers. With the continuous increase in the number of SVM classifiers, the MCRSVMC algorithm classification ACC showed a trend of increasing first and then decreasing (Figure 5). When the number of SVM classifiers was 410, the classification ACC of the MCRSVMC algorithm reached the maximum value (0.9429).

Further analysis of the optimal feature subset (Figure 6) revealed that, as the number of important features continued to increase, the MCRSVMC algorithm classification ACC showed a trend of increase first and then decrease. When the number of important features was 260, the classification ACC of the MCRSVMC algorithm reached the maximum value (0.9092).

3.3. Abnormal Brain Areas in CIS Patients. Based on the classification method of the MCRSVMC algorithm, the abnormal brain areas of CIS patients were analyzed (Figure 7). The analysis results revealed that the abnormal brain areas of CIS patients were mainly distributed in the temporal pole: the middle temporal gyrus (TPOMid.L), the superior temporal gyrus (STG.L), posterior cingulate gyrus (PCG.L), parahippocampal gyrus (PHG.R), middle frontal

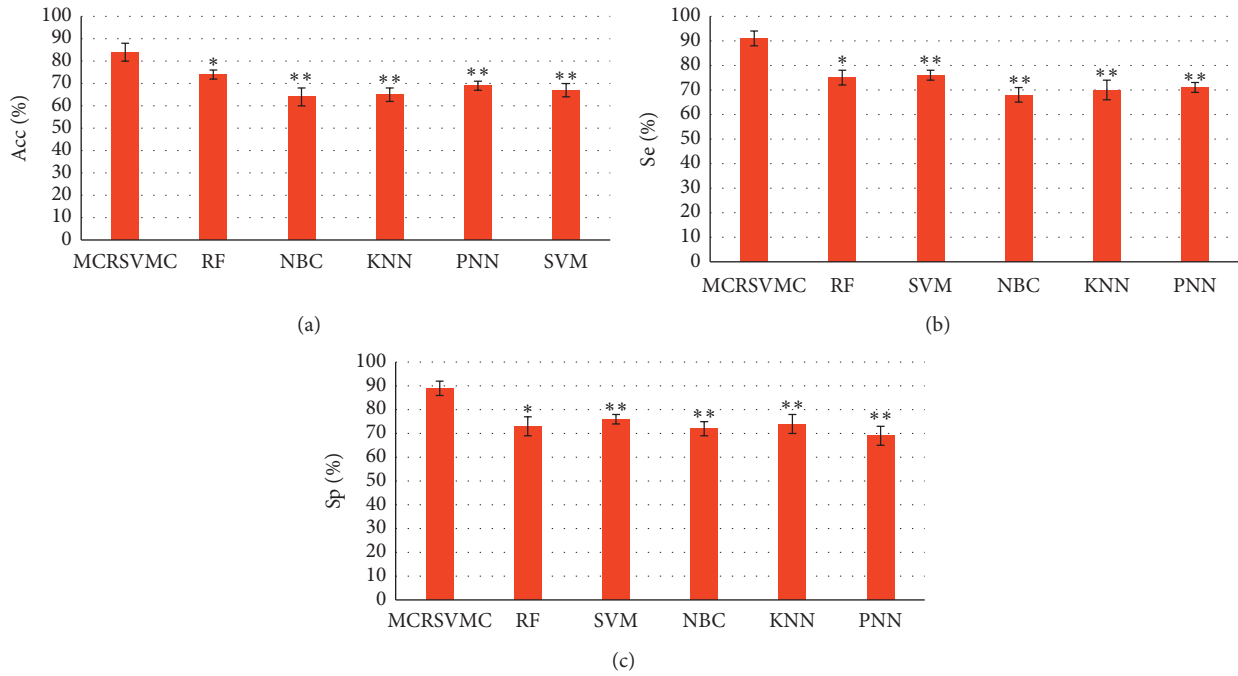


FIGURE 3: Comparison on classification performances of different algorithms. (a–c) Comparison results of ACC, SEN, and SPE of different algorithms, respectively. * and ** indicated that the difference was statistically obvious ($P < 0.05$) and extremely statistically obvious ($P < 0.01$) in contrast to the MCRSVMC algorithm, respectively.

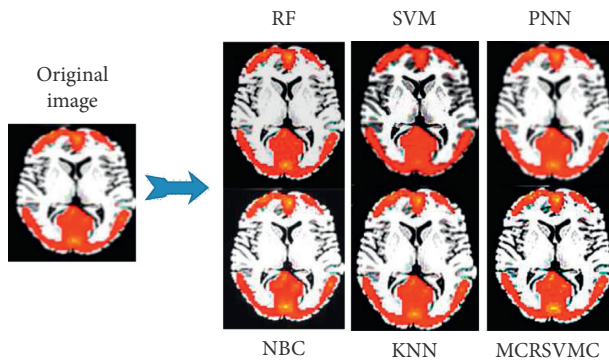


FIGURE 4: Display of image processing effects by different algorithms.

gyrus (MFG.L), Rolandic operculum (ROL.R), inferior temporal gyrus (ITG.R), and fusiform gyrus (FFG.L).

3.4. Comparison on the Basic Data of Patients in Two Groups.

The age, gender ratio, body mass index (BMI), course of the disease, heterogeneity index score (HIS), and MoCA score of the two groups of patients were compared, and the results are given in Table 1. The age, gender ratio, BMI, course of the disease, HIS, and MoCA score of the two groups before treatment were not statistically different ($P > 0.05$).

3.5. Comparison of Neuropsychological Scales between the Two Groups of Patients after Treatment. The MoCA scores, LOTCA scores, and FIM scores of the two groups of patients before and after treatment are compared in Figure 8, which

suggested that there was no obvious difference before treatment ($P > 0.05$). After treatment, the MoCA scores of the two groups of patients were increased, showing statistically great difference ($P < 0.05$); the LOTCA scores and FIM scores of the two groups of patients were extremely increased in contrast to those before the treatment, showing statistically great differences ($P < 0.01$). In addition, the MoCA score, LOTCA score, and FIM score of the intervention group (23.99 ± 0.28 ; 90.12 ± 5.44 ; 102.64 ± 2.49) were higher than those of the control group (25.91 ± 1.17 ; 98.17 ± 4.92 ; 114.27 ± 2.59) after the treatment ($P < 0.05$).

3.6. Comparison on the ReHo Value of Patients before and after the Treatment. The comparison on the ReHo value of the intervention group and the control group before treatment showed that the increased brain areas included the left dorsolateral superior frontal gyrus and the left middle frontal gyrus, and the decreased brain areas were the right posterior cingulate gyrus and the left parahippocampal gyrus. However, there was no statistical difference in the ReHo value between the two groups ($P > 0.05$) (Table 2 and Figure 9).

In the control group, the brain areas with increased ReHo values after treatment included the left parahippocampal gyrus, right temporal polar area, and right middle frontal gyrus, while the brain areas with decreased ReHo values included the bilateral inferior frontal gyrus and left lateral central posterior back (Table 3 and Figure 10). The ReHo values of different brain regions were statistically different compared with those before treatment ($P < 0.05$).

In the intervention group, the brain regions with increased ReHo values after treatment compared with before

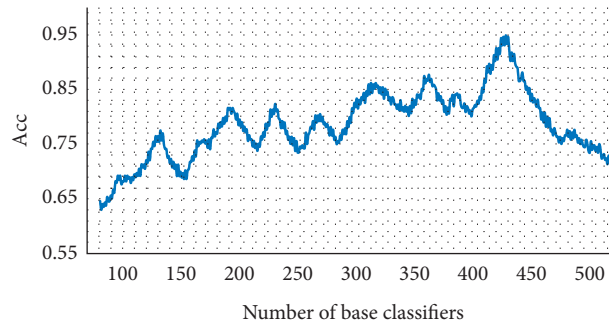


FIGURE 5: Selection of the optimal number of classifiers.

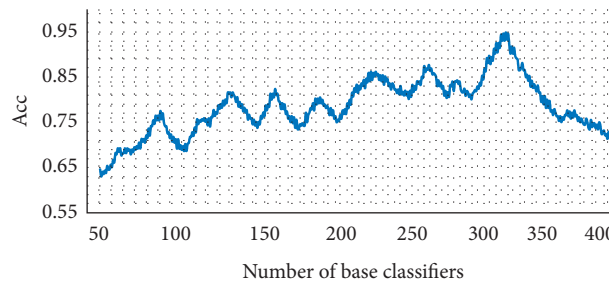


FIGURE 6: Selection of the optimal feature subset.

treatment included the left parahippocampal gyrus, left middle temporal gyrus, right temporal polar region, and right central anterior gyrus, while the brain regions with decreased ReHo values included the right-side inferior temporal gyrus, left inferior frontal gyrus, and right inferior frontal gyrus (Table 4 and Figure 11). The ReHo values of different brain regions were statistically different compared with those before treatment ($P < 0.05$). After treatment, the intervention group only had brain areas with increased ReHo values in the right inferior temporal gyrus and the right inferior frontal gyrus in contrast to the control group, showing statistical differences between the two ($P < 0.05$).

4. Discussion

After adopting the MCRSVMC algorithm, the diagnosis and treatment effect evaluation of patients with cognitive dysfunction after CIS showed that the average classification ACC, SEN, and SPE of the MCRSVMC algorithm were $84.25 \pm 4.13\%$, $91.07 \pm 3.51\%$, and $89. \pm 3.96\%$, respectively, which were all much better than those of other algorithms ($P < 0.01$). Wu et al. [10] used the SVM of 9 connected feature subsets to classify the patients with different degrees of cognitive dysfunction and found that the classification ACC was 63.4%. Long et al. [11] used the multicore SVM algorithm to classify the patients with different degrees of cognitive dysfunction, reaching the ACC of 78.8%. Therefore, the classification ACC of the MCRSVMC algorithm in this study was obviously better than that of the current algorithms.

In this study, drug therapy and acupuncture were used to treat patients with cognitive dysfunction after CIS. The results showed that, after treatment, the MoCA score,

LOTCA score, and FIM score of the intervention group (23.99 ± 0.28 ; 90.12 ± 5.44 ; 102.64 ± 2.49) were higher than those of the control group (25.91 ± 1.17 ; 98.17 ± 4.92 ; 114.27 ± 2.59) ($P < 0.05$). The ReHo values of the right inferior temporal gyrus and right inferior frontal gyrus of patients in the intervention group were much higher in contrast to those of the control group ($P < 0.05$). These results indicated that acupuncture could greatly improve the cognitive dysfunction of patients. Acupuncture can not only promote the regeneration and repair of synapses and improve the function of the central nervous system [12] but also stimulate the cerebral cortex through the skull, improve the brain function under pathological conditions [13], and promote the cortex around the cerebral ischemic area. The high expression of synaptophysin accelerates the reconstruction of nerve function [14]. Current research results show that human cognitive function is highly correlated with the cortex such as the frontal lobe, temporal lobe, and parietal lobe [15]. Li et al. [16] pointed out that acupuncture treatment could effectively improve the cerebral hemodynamics of patients and found that ReHo of the right posterior cingulate gyrus and left parahippocampal gyrus of the two groups of patients before treatment decreased, suggesting that the nerves' meta-excitability was decreased, and the local brain function activities were reduced, which indicated that ischemic damage to the cingulate gyrus and parahippocampal gyrus can lead to cognitive dysfunction [17]. The increase of ReHo in the left dorsolateral superior frontal gyrus brain area indicates that these brain areas are a functional compensation for the damaged brain area [18]. After treatment, ReHo values in the left parahippocampal gyrus, right middle frontal gyrus, and right temporal pole brain area increased in the two groups of

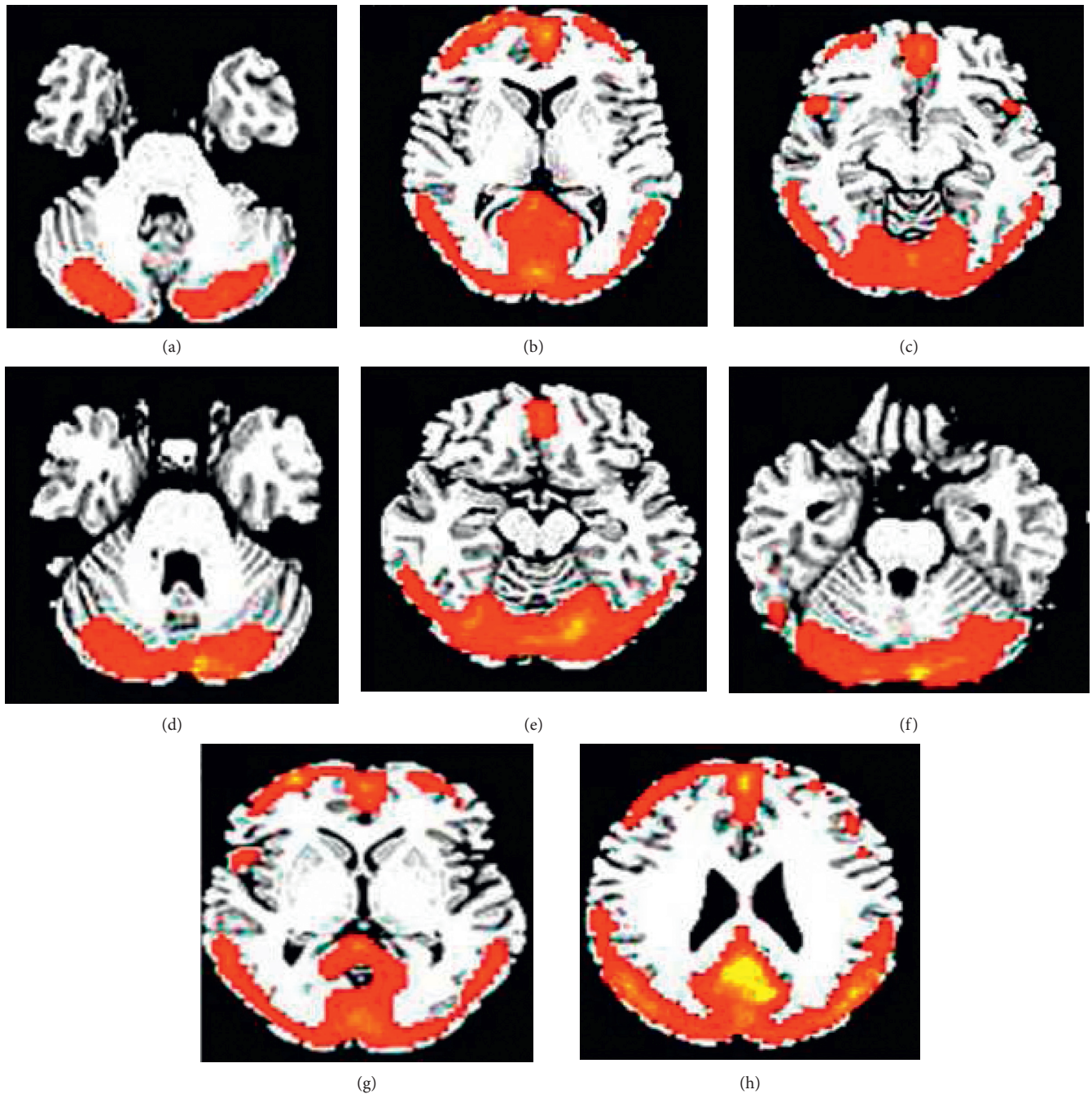


FIGURE 7: Distribution of abnormal brain areas of CIS patients. (a–h) The distributions of TPOmid.L, STG.L, PCG.L, PHG.R, MFG.L, ROL.R, ITG.R, and FFG.L, respectively.

TABLE 1: Comparison on the basic data of patients in two groups.

Item	Control group ($n = 18$)	Intervention group ($n = 18$)	t value or χ^2 value	P value
Age (years)	63.06 ± 3.85	63.91 ± 3.27	0.363	0.745
Males (cases, (%))	11 (30.56)	9 (25)	1.002	0.877
BMI (kg/m^2)	25.19 ± 2.08	24.95 ± 3.19	1.307	0.161
Course of the disease (months)	5.76 ± 1.28	4.92 ± 2.03	0.684	0.532
HIS score	8.94 ± 0.99	9.23 ± 1.02	0.772	0.447
MoCA score	22.32 ± 2.09	22.40 ± 1.13	1.348	0.191

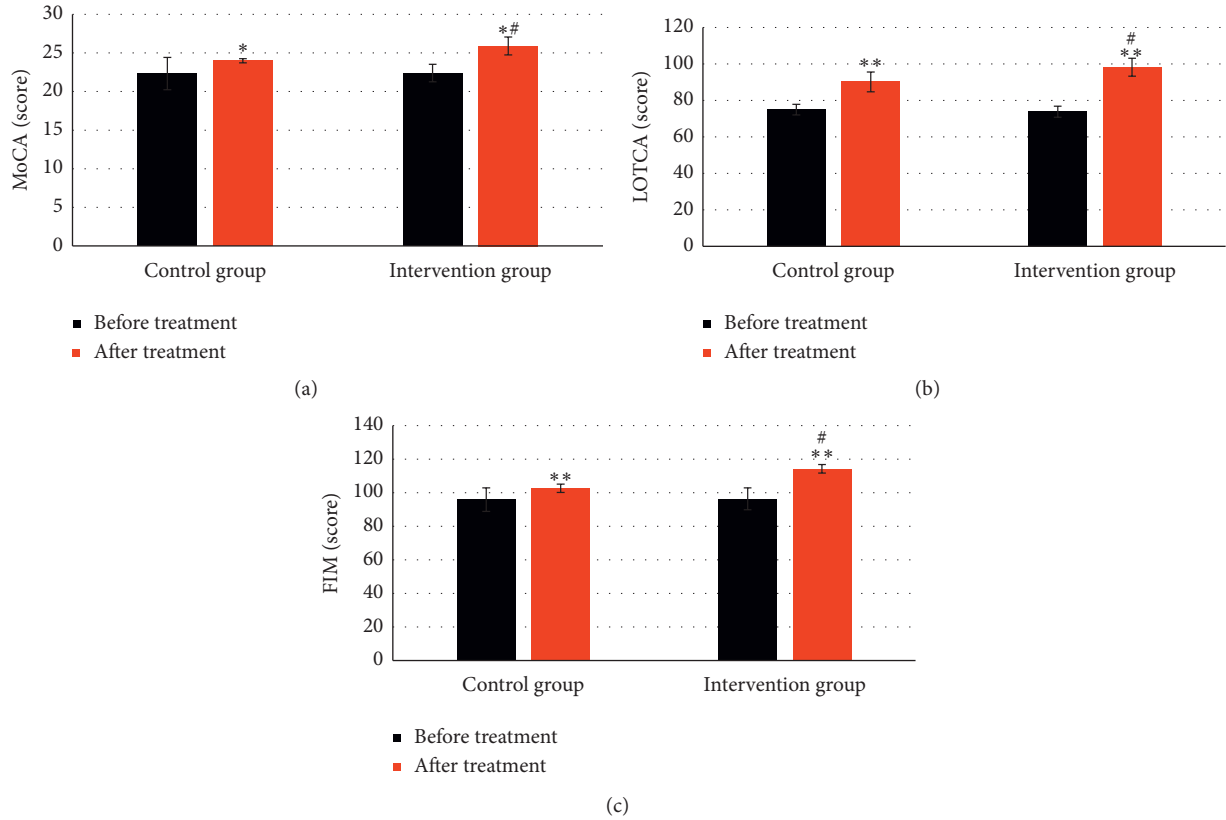


FIGURE 8: Comparison of neuropsychological scales between the two groups of patients after treatment. (a–c) Comparison results of the MoCA score, LOTCA score, and FIM score, respectively. * and # suggested that the difference was statistically observable in contrast to the score before the treatment and the control group, respectively ($P < 0.05$); ** indicated that the difference was extremely great statistically in contrast to the score before the treatment ($P < 0.01$).

TABLE 2: Brain areas with changed ReHo before the treatment of patients in two groups.

	Brain area (AAL format)	Coordinate			Number of voxels	<i>t</i> value
		<i>X</i>	<i>Y</i>	<i>Z</i>		
Increased	Left dorsolateral upper frontal gyrus	-27	-3	75	15	7.1422
	Left middle frontal gyrus	-39	21	36	17	2.7238
	Right posterior cingulate gyrus	9	-48	12	10	-7.2517
Decreased	Left hippocampal gyrus	-15	-36	-9	12	-6.5426
	Left lower frontal gyrus	-15	15	-18	20	-2.9182

patients, and ReHo values in the right inferior temporal gyrus and right inferior frontal gyrus increased more in the intervention group. Such results indicated that the two treatment

methods could improve the brain function of the damaged brain area, and acupuncture can improve the cognitive dysfunction more obviously.

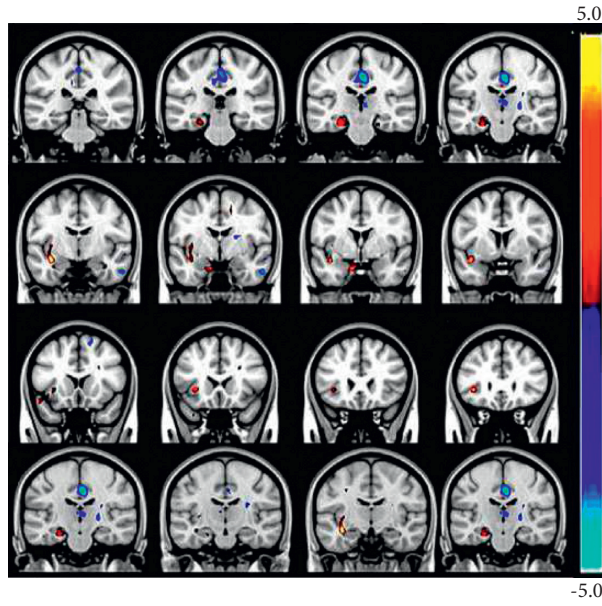


FIGURE 9: Brain areas with changed ReHo before the treatment.

TABLE 3: Brain areas with changed ReHo after the treatment of patients in the control group.

	Brain area (AAL format)	Coordinate			Number of voxels	<i>t</i> value
		<i>X</i>	<i>Y</i>	<i>Z</i>		
Increased	Left hippocampal gyrus	-27	-30	-25	55	3.0221
	Right middle frontal gyrus	48	39	10	54	2.8894
	Right temporal pole	30	9	-40	51	2.2910
Decreased	Left central posterior back	-47	-25	8	52	-4.9602
	Left lower forehead left	-21	24	-20	70	-5.6895
	Right lower forehead left	18	30	-23	71	-5.7874

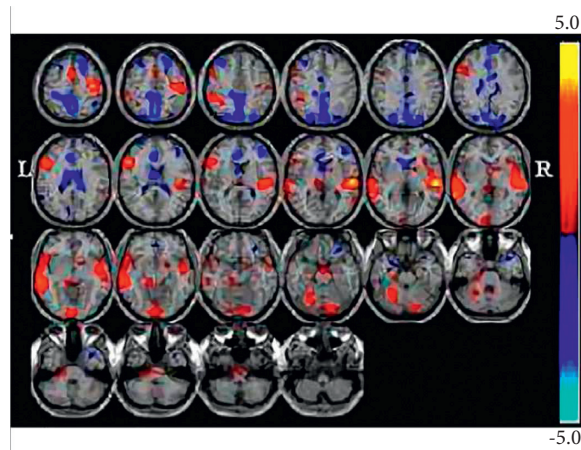


FIGURE 10: Brain areas with changed ReHo of patients in the control group after the treatment.

TABLE 4: Brain areas with changed ReHo after the treatment of patients in the intervention group.

	Brain area (AAL format)	Coordinate			Number of voxels	<i>t</i> value
		<i>X</i>	<i>Y</i>	<i>Z</i>		
Increased	Left parahippocampal gyrus	-27	-30	-25	56	8.0014
	Left middle temporal gyrus	-42	-71	23	75	4.8185
	Right temporal polar region	53	9	10	51	4.1582
	Right central anterior gyrus	21	10	71	64	5.8658
Decreased	Right-side inferior temporal gyrus	18	30	-23	58	-6.2876
	Left inferior frontal gyrus	-21	24	-20	45	-5.7753
	Right inferior frontal gyrus	18	30	-23	60	-6.1987

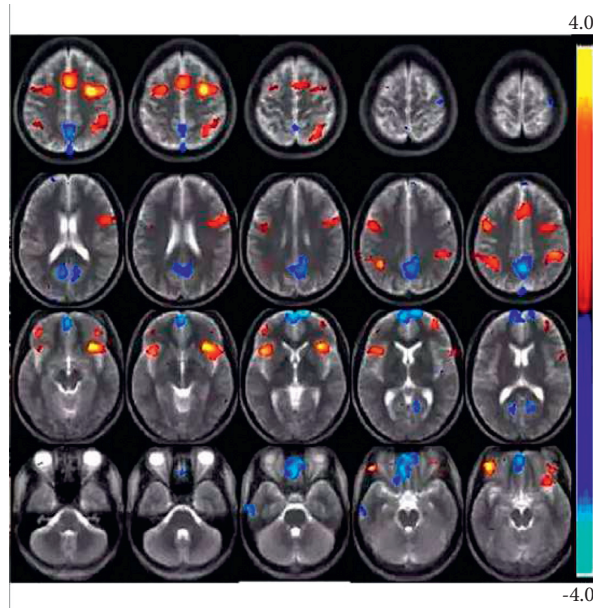


FIGURE 11: Brain areas with changed ReHo of patients in the intervention group after the treatment.

5. Conclusion

Based on the MCRSVMC algorithm, a fMRI image brain region classification model was constructed and applied to the diagnosis and efficacy evaluation of patients with cognitive dysfunction after CIS. The results showed that the fMRI image brain region classification model based on the MCRSVMC algorithm significantly improved the brain region classification ACC, SPE, and SEN. However, there were some shortcomings. It only evaluated the ReHo values of BOLD-fMRI and failed to analyze the low-frequency oscillation amplitude and functional connectivity. In the future work, it would continue to analyze the impacts of different treatments based on the MCRSVMC algorithm on the BOLD-fMRI-related parameters. In summary, the ACC, SPE, and SEN of the MRI image classification model based on the MCRSVMC algorithm in this study were greatly improved, and acupuncture showed a better therapeutic effect on patients with cognitive dysfunction after CIS. The results could provide a basis for reference for the clinical diagnosis and treatment of ischemic stroke.

Data Availability

The data used to support the findings of this study are available from the corresponding author upon request.

Conflicts of Interest

The authors declare no conflicts of interest.

References

- [1] T. Chiasakul, E. De Jesus, J. Tong et al., "Inherited thrombophilia and the risk of arterial ischemic stroke: a systematic review and meta-analysis," *Journal of the American Heart Association*, vol. 8, no. 19, Article ID e012877, 2019.
- [2] Z. Lv and W. Xiu, "Interaction of edge-cloud computing based on SDN and NFV for next generation IoT," *IEEE Internet of Things Journal*, vol. 7, no. 7, pp. 5706–5712, 2020.
- [3] N. Kagiya, S. Shrestha, P. D. Farjo, and P. P. Sengupta, "Artificial intelligence: practical primer for clinical research in cardiovascular disease," *Journal of the American Heart Association*, vol. 8, no. 17, Article ID e012788, 2019.

- [4] C. Guo, J. Lu, Z. Tian, W. Guo, and A. Darvishan, "Optimization of critical parameters of PEM fuel cell using TLBO-DE based on Elman neural network," *Energy Conversion and Management*, vol. 183, no. MAR., pp. 149–158, 2019.
- [5] C. Krittanawong, K. W. Johnson, R. S. Rosenson et al., "Deep learning for cardiovascular medicine: a practical primer," *European Heart Journal*, vol. 40, no. 25, pp. 2058–2073, 2019.
- [6] A. Maier, C. Syben, T. Lasser, and C. Riess, "A gentle introduction to deep learning in medical image processing," *Zeitschrift für Medizinische Physik*, vol. 29, no. 2, pp. 86–101, 2019.
- [7] Z. Sun, Y. Qiao, B. P. F. Lelieveldt, and M. Staring, "Integrating spatial-anatomical regularization and structure sparsity into SVM: i," *NeuroImage*, vol. 178, pp. 445–460, 2018.
- [8] Y. Chen, S. Hu, H. Mao, W. Deng, and X. Gao, "Application of the best evacuation model of deep learning in the design of public structures," *Image and Vision Computing*, vol. 102, Article ID 103975, 2020.
- [9] S. H. Hojjati, A. Ebrahimzadeh, A. Khazaei, and A. Babajani-Feremi, "Predicting conversion from MCI to AD using resting-state fMRI, graph theoretical approach and SVM," *Journal of Neuroscience Methods*, vol. 282, pp. 69–80, 2017.
- [10] Y. Wu, T. Li, Y. Han, and J. Jiang, "Use of radiomic features and support vector machine to discriminate subjective cognitive decline and healthy controls," *Annual International Conference of the IEEE Engineering in Medicine & Biology Society (EMBC)*, vol. 2020, Article ID 9175840, 1765 pages, 2020.
- [11] Z. Long, B. Jing, H. Yan et al., "A support vector machine-based method to identify mild cognitive impairment with multi-level characteristics of magnetic resonance imaging," *Neuroscience*, vol. 331, pp. 169–176, 2016.
- [12] Y. S. Ho, F. Y. Zhao, W. F. Yeung, G. T. Wong, H. Q. Zhang, and R. C. Chang, "Application of acupuncture to attenuate immune responses and oxidative stress in postoperative cognitive dysfunction: what do we know so far?," *Oxid Med Cell Longev*, vol. 2020, Article ID 9641904, 2020.
- [13] X. Gao and J. Cai, "Optimization analysis of urban function regional planning based on big data and gis technology," *Boletín Tecnico/Technical Bulletin*, vol. 55, no. 11, pp. 344–351, 2017.
- [14] Y. Tang, T. Wang, L. Yang et al., "Acupuncture for postoperative cognitive dysfunction: a systematic review and meta-analysis of randomized controlled trials," *Acupuncture in Medicine*, vol. 42, Article ID 096452842096139, 2020.
- [15] X. Su, Z. Wu, F. Mai et al., "Governor vessel-unblocking and mind-regulating' acupuncture therapy ameliorates cognitive dysfunction in a rat model of middle cerebral artery occlusion," *International Journal of Molecular Medicine*, vol. 43, no. 1, pp. 221–232, 2019.
- [16] W. Li, Q. Wang, S. Du, Y. Pu, and G. Xu, "Acupuncture for mild cognitive impairment in elderly people," *Medicine*, vol. 99, no. 39, Article ID e22365, 2020.
- [17] H.-W. Suh, J. Kim, O. Kwon et al., "Neurocircuitry of acupuncture effect on cognitive improvement in patients with mild cognitive impairment using magnetic resonance imaging: a study protocol for a randomized controlled trial," *Trials*, vol. 20, no. 1, p. 310, 2019.
- [18] M. S. Jung, M. Zhang, M. K. Askren et al., "Cognitive dysfunction and symptom burden in women treated for breast cancer: a prospective behavioral and fMRI analysis," *Brain Imaging and Behavior*, vol. 11, no. 1, pp. 86–97, 2017.